PRAMANA
— journal of
physics

Vol. 60, No. 1
January 2003
pp. 123–141

Strain field due to transition metal impurities in Ni and Pd

HITESH SHARMA[1,*] and S PRAKASH[2]
[1]Department of Physics, Panjab University, Chandigarh 160 014, India
[2]Jiwaji University, Gwalior 474 011, India
[*]Email: hitesh10@mailcity.com

MS received 17 January 2002; revised 1 August 2002

Abstract. The strain field due to body centered substitutional transition metal impurities in Ni and Pd metals are investigated. The calculations are carried out in the discrete lattice model of the metal using Kanzaki lattice static method. The effective ion–ion interaction potential due to Wills and Harrison is used to evaluate dynamical matrix and the impurity-induced forces. The results for atomic displacements due to 3d, 4d and 5d impurities (Fe, Co, Cu, Nb, Mo, Pd, Pt and Au) in Ni and (Fe, Co, Cu, Ni, Nb, Mo, Pt and Au) impurities in Pd are given up to 25 NN's of impurity and these are compared with the available experimental data. The maximum displacements of 4.6% and 3.8% of 1NN distance are found for NiNb and PdNb alloys respectively, while the minimum displacements of 0.63% and 0.23% of 1NN distance are found for NiFe and PdFe alloys respectively. Except for Cu, the atomic displacements are found to be proportional to the core radii and d state radius. The relaxation energies for 3d impurities are found less than those for 4d and 5d impurities in Ni and Pd metals. Therefore, 3d impurities may easily be solvable in these metals.

Keywords. Strain field; point defects; transition metal based dilute alloys.

PACS Nos 61.72.-y; 61.72.Ji; 61.43.-j; 61.72.Bb

1. Introduction

We had used the Kanzaki lattice static method to investigate the strain field due to transition metal impurities in bcc transition metals vanadium and iron [1,2]. The effective ion–ion interaction potential due to Wills and Harrison [3] was used to calculate the Kanzaki forces. The calculated atomic displacements of NN's of impurities in V host exhibited the same trend as predicted by X-ray diffraction studies for the fractional change in the lattice parameter. Since the data of atomic displacements calculated in the discrete lattice model are of vital importance to study the elastic and electronic properties of dilute alloys [4–7], it is interesting to report the calculations for strain field due to transition metal impurities in fcc Ni and Pd using discrete lattice model. The paper is organized as follows: The necessary formalism is given in §2, the calculations and results are presented in §3 and these are discussed in §4.

2. Formalism

For a perfect crystal with self consistent pair potential $\phi(r)$, the total interaction energy Φ_0 is given as

$$\Phi_0 = \sum_n \phi(\vec{R}_n^0) \tag{1}$$

where $\vec{R}_n^0$ is the equilibrium position of the nth host atom. If an impurity is introduced at the origin, the lattice gets strained, and the host atoms move to new equilibrium positions $\vec{R}_n = \vec{R}_n^0 + \vec{u}(\vec{R}_n^0)$, where $\vec{u}(\vec{R}_n^0)$ are the atomic displacements. Kanzaki assumed that these atomic displacements are produced by an appropriate distribution of external forces in the crystal which depend upon the nature of the impurity. The potential energy of the strained lattice under applied external forces is expanded in powers series of the displacements which in the harmonic approximation is given as

$$\Phi = \Phi_0 - \sum_{n,\alpha} u_\alpha(\vec{R}_n^0) F_\alpha(\vec{R}_n^0) + \frac{1}{2} \sum_{n,\alpha} \sum_{n',\beta} u_\alpha(\vec{R}_n^0) u_\beta(\vec{R}_{n'}^0) \phi_{\alpha\beta}(n,n') \tag{2}$$

where Φ_0 is the potential energy of the perfect lattice, the force components

$$F_\alpha(\vec{R}_n^0) = -\left.\frac{\partial \Phi}{\partial u_\alpha(\vec{R}_n^0)}\right|_{u_\alpha(\vec{R}_n^0)=0} \tag{3}$$

and the force constants

$$\phi_{\alpha\beta}(n,n') = \left.\frac{\partial^2 \Phi}{\partial u_\alpha(\vec{R}_n^0) \partial u_\beta(\vec{R}_{n'}^0)}\right|_{u_\alpha(\vec{R}_n^0)=u_\beta(\vec{R}_{n'}^0)=0}. \tag{4}$$

Here $\alpha, \beta(x,y,z)$ denote the Cartesian components, $F_\alpha(\vec{R}_n^0)$ is the α component of the external force applied on the atom R_n^0 and $\phi_{\alpha\beta}(n,n')$ are the force constants which obey the crystal symmetries. The equilibrium values of $u(R_n^0)$ are obtained by minimizing Φ with respect to $u_\alpha(R_n^0)$, i.e.,

$$\frac{\partial \Phi}{\partial u_\alpha(R_n^0)} = 0. \tag{5}$$

Substituting eq. (2) in (5), one finds

$$F_\alpha(\vec{R}_n^0) = \sum_{n',\beta} \phi_{\alpha\beta}(n,n') u_\beta(\vec{R}_{n'}^0). \tag{6}$$

Evidently the displacements can be evaluated if $F_\alpha(\vec{R}_n^0)$ and $\phi_{\alpha\beta}(n,n')$ are known.

In the Kanzaki lattice static method the displacements are expanded in normal coordinates as

$$u_\alpha(\vec{R}_n^0) = \sum_{\vec{q}} Q_\alpha(\vec{q}) \exp(\imath \vec{q} \cdot \vec{R}_n^0) \tag{7}$$

where $\vec{q}$ is a wave vector and the expansion coefficients $\vec{Q}(\vec{q})$ are normal coordinates. Since we are considering a periodic superlattice of defects, the wave vectors $\vec{q}$ must satisfy periodic boundary conditions, and all such physically distinct $\vec{q}$ vectors will be contained within the first Brillouin zone. $\vec{Q}(\vec{q})$ are in general, complex and, to ensure the reality condition for displacements

$$\vec{Q}(-\vec{q}) = \vec{Q}^*(\vec{q}), \tag{8}$$

where the asterisk stands for the complex conjugate. Using eq. (7) in eq. (2), one gets the Fourier transform of the total energy Φ of the strained lattice as

$$\Phi = \Phi_0 - \sum_{\alpha q} F_\alpha(\vec{q}) Q_\alpha(\vec{q}) + \frac{N}{2} \sum_{\alpha\beta} \sum_{q} \phi_{\alpha\beta}(\vec{q}) Q_\alpha(\vec{q}) Q_\beta(\vec{q}) \tag{9}$$

where

$$F_\alpha(\vec{q}) = \sum_n F_\alpha(\vec{R}_n^0) \exp(\imath \vec{q} \cdot \vec{R}_n^0), \tag{10}$$

and

$$\phi_{\alpha\beta}(\vec{q}) = \sum_{n-n'} \phi_{\alpha\beta}(n-n') \exp\left[-\imath \vec{q} \cdot (\vec{R}_n^0 - \vec{R}_{n'}^0)\right]. \tag{11}$$

N is the number of unit cells in the crystal and $F_\alpha(\vec{q})$ and $\phi_{\alpha\beta}(\vec{q})$ are the Fourier transforms of $F_\alpha(\vec{R}_n^0)$ and $\phi_{\alpha\beta}(n-n')$, respectively. The equilibrium condition in Fourier space becomes

$$\frac{\partial \Phi}{\partial Q_\alpha(q)} = 0 \tag{12}$$

which in conjuntion with eq. (9) gives

$$\sum_\beta \left[N \phi_{\alpha\beta}(-\vec{q}) Q_\beta(\vec{q}) - F_\beta(\vec{q}) \delta_{\alpha\beta} \delta_{-\vec{q},\vec{q}} \right] = 0. \tag{13}$$

Equation (13) gives three simultaneous equations for three components $Q_\beta(\vec{q})$ for each value of $\vec{q}$. If $\phi_{\alpha\beta}(\vec{q})$ and $F_\beta(\vec{q})$ are known, eq. (13) can be solved for $\vec{Q}(\vec{q})$ which, in turn, gives $u_\alpha(\vec{R}_n^0)$ from eq. (7).

For a central ion–ion potential, the dynamical matrix is written as

$$\phi_{\alpha\beta}(n) = \left.\frac{\partial^2 \phi}{\partial r_\alpha \partial r_\beta}\right|_{r=R_n^0} = \frac{R_{n\alpha}^0 R_{n\beta}^0}{|\vec{R}_n^0|^2} (A_n - B_n + \delta_{\alpha\beta} B_n), \tag{14}$$

where

$$A_n = \left.\frac{\partial^2 \phi}{\partial r^2}\right|_{r=R_n^0}, \quad B_n = \frac{1}{|\vec{R}_n^0|} \left.\frac{\partial \phi}{\partial r}\right|_{r=R_n^0}. \tag{15}$$

In the metallic crystal, the ions are screened by the conduction electrons thereby decreasing the ionic potential faster, which exhibit oscillatory behavior at large distances. It has been found that in the d-band metals the screening is large [9,10]. Therefore, the major contribution to $\phi_{\alpha\beta}(\vec{q})$ and $F_\alpha(\vec{q})$ in these metals is expected to arise from the first few NN's. Including the interactions up to 1NN's, $\phi_{\alpha\beta}(\vec{q})$ for the fcc structure, from eqs (11) and (14) becomes

$$\phi_{\alpha\alpha}(\vec{q}) = 2(A_1 + B_1)\left\{1 - \cos\left(\frac{q_\alpha a}{2}\right)\left[\cos\left(\frac{q_\beta a}{2}\right) + \cos\left(\frac{q_\gamma a}{2}\right)\right]\right\} \tag{16}$$

$$\phi_{\alpha\beta}(\vec{q}) = 2(A_1 - B_1)\left[\sin\left(\frac{q_\alpha a}{2}\right) + \sin\left(\frac{q_\beta a}{2}\right)\right], \tag{17}$$

where $\alpha \neq \beta \neq \gamma$ and a is the lattice parameter. Similarly, eq. (10) at the 1NN shell of impurity gives

$$F_\alpha(\vec{q}) = i2\sqrt{2}F_{\mathrm{I}}\sin\left(\frac{q_\alpha a}{2}\right)\left[\cos\left(\frac{q_\beta a}{2}\right)\cos\left(\frac{q_\gamma a}{2}\right)\right], \tag{18}$$

where F_{I} is the force acting on the 1NN sites of impurity. Considering the interaction with the 2NN shell, the components of $F(\vec{q})$ are

$$F_\alpha(\vec{q}) = i2F_{\mathrm{II}}\sin(q_\alpha a), \tag{19}$$

where F_{II} is the force at the 2NN site of impurity.

With the knowledge of $\phi_{\alpha\beta}(q)$ and $F_\alpha(q)$, one can solve eq. (13) for $\vec{Q}(\vec{q})$ using the properties of determinants. For the radial forces at the 1NN's shell only (usually called the F_{I} system) of the impurity,

$$\imath Q_1(q) = \frac{\sqrt{2}F_{\mathrm{I}}}{NA_1}\frac{\begin{vmatrix}\sin x(\cos y + \cos z) & G_2 & G_3\\ \sin y(\cos z + \cos x) & G_{22} & G_4\\ \sin z(\cos x + \cos y) & G_4 & G_{33}\end{vmatrix}}{\Delta}, \tag{20}$$

where

$$\Delta = \begin{vmatrix}G_{11} & G_2 & G_3\\ G_2 & G_{22} & G_4\\ G_3 & G_4 & G_{33}\end{vmatrix}, \tag{21}$$

$$G_{11} = \left[1 + \frac{B_1}{A_1}\right][2 - \cos x(\cos y + \cos z)], \tag{22}$$

$$G_2 = \left[1 - \frac{B_1}{A_1}\right]\sin x \sin y, \tag{23}$$

$$G_3 = \left[1 - \frac{B_1}{A_1}\right] \sin x \sin z, \tag{24}$$

$$G_4 = \left[1 - \frac{B_1}{A_1}\right] \sin y \sin z, \tag{25}$$

$$x = \frac{q_x a}{2}, \quad y = \frac{q_y a}{2}, \quad z = \frac{q_z a}{2}. \tag{26}$$

G_{22} and G_{33} are obtained from the expression for G_{11} by cyclic permutation of x, y, z. $Q_2(q)$ and $Q_3(q)$ can be obtained from $Q_1(q)$ using cubic symmetry. For the radial forces acting only on the 2NN shell (called F_{II} system) of the impurity,

$$\imath Q_1 = \frac{F_{\mathrm{II}}}{NA_1} \begin{vmatrix} \sin 2x & G_2 & G_3 \\ \sin 2y & G_{22} & G_4 \\ \sin 2z & G_4 & G_{33} \end{vmatrix}. \tag{27}$$

$Q_2(q)$ and $Q_3(q)$ can be obtained from $Q_1(q)$ using cubic symmetry.

2.1 *Calculation of F_{I} and F_{II}*

The external force $\vec{F}(R_n^0)$ for substitutional impurity in fcc host is calculated considering the four configurations as shown in figure 1. The difference in the potential energies of the (a) and (d) configurations is

$$\begin{aligned} \Phi(d) - \Phi(a) &= [\Phi(d) - \Phi(c)] + [\Phi(c) - \Phi(b)] + [\Phi(b) - \Phi(a)] \\ &= \sum_n [\phi_{\mathrm{IH}}(|\vec{R}_n|) - \phi_{\mathrm{HH}}(|\vec{R}_n|)] \\ &\quad + \frac{1}{2} \sum_{n,n'} [\phi_{\mathrm{HH}}(|\vec{R}_{n'} - \vec{R}_n|) - \phi_{\mathrm{HH}}(|\vec{R}_{n'}^0 - \vec{R}_n^0|)], \end{aligned} \tag{28}$$

where $\phi_{\mathrm{HH}}(r)$ and $\phi_{\mathrm{IH}}(r)$ are the host–host and impurity–host interaction potentials respectively. Comparing eqs (2) and (28), the second term of both the expression is the same. Therefore, equating the first term of eqs (2) and (28), one gets

$$F_\alpha(\vec{R}_n^0) = -\frac{\partial}{\partial u_\alpha(R_n^0)} \sum_{n'} \Delta\phi(|\vec{R}_{n'}|) \tag{29}$$

where

$$\Delta\phi(r) = \phi_{\mathrm{IH}}(r) - \phi_{\mathrm{HH}}(r). \tag{30}$$

Expanding $\Delta\phi(|\vec{R}_{n'}|)$ in the power series of $\vec{u}(\vec{R}_n^0)$, the forces F_{I} and F_{II} for the central potential are given as

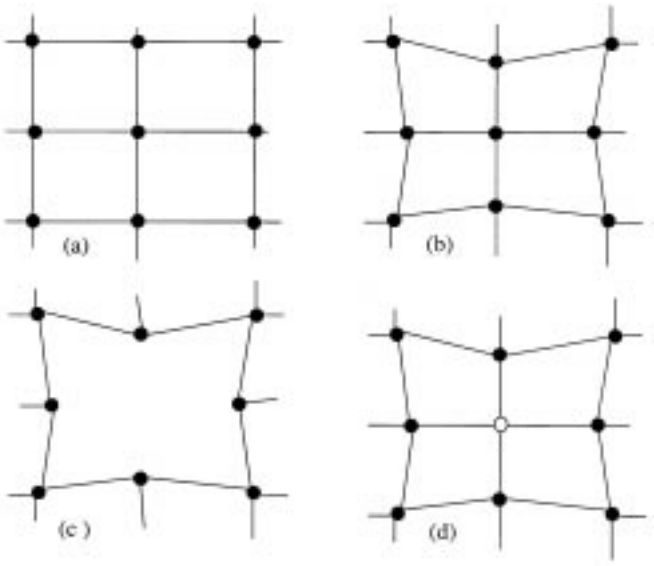

Figure 1. The four configurations of the lattice for substitutional impurity. (**a**) Perfect host lattice, (**b**) strained lattice due to external force, (**c**) strained lattice with one atom removed, and (**d**) an impurity atom placed at the vacant lattice site.

$$F_\alpha(\vec{R}_n^0) = -\frac{\partial}{\partial r}\Delta\phi\bigg|_{|r|=|\vec{R}_n^0|} - \vec{u}(\vec{R}_n^0)\frac{\partial^2}{\partial r^2}\Delta\phi\bigg|_{|r|=|\vec{R}_n^0|}. \tag{31}$$

Equation (31) can be solved in the two approximations. If $u(R_n^0)$ is very small, the second term in eq. (31) can be neglected. It is called the first approximation where the force constants of the host metal remain unchanged in the presence of the impurity. If $u(R_n^0)$ is significant, both the terms in eq. (31) are retained. It is called the second approximation and takes care of the impurity-induced change in the force constants of the lattice. To include the interactions up to 2NN's, the atomic displacements due to $F_{\rm I}$ and $F_{\rm II}$ are combined to evaluate $\vec{u}(\vec{R}_n^0)$ in the second approximation as done by Kanzaki [11].

The conduction electrons in the transition metal have both the s and quasilocalized d character and these characteristics should be included in the calculation of the ion–ion interaction potential. In the formation of TM, d state are broadened into quasilocalized bands with finite bandwidth. Further, the d bands get distorted due to crystal potential and there is s–d hybridization. These effects are included in the Wills and Harrison transition metal model potential [2] which is given as

$$\phi_{\rm HH}(r) = \phi_{\rm HH}^{\rm FE}(r) + \phi_{\rm HH}^{c}(r) + \phi_{\rm HH}^{b}(r), \tag{32}$$

where

$$\phi_{\rm HH}^{\rm FE}(r) = Z_{\rm sH}^2 e^2 \cosh^2(\kappa r_{\rm cH})\frac{\exp(-\kappa r)}{r} \tag{33}$$

$$\phi_{\rm HH}^{c}(r) = Z_{\rm dH}\frac{225}{\pi^2}\frac{\hbar^2 r_{\rm dH}^6}{m r^8} \tag{34}$$

and

$$\phi^{b}_{\mathrm{HH}}(r) = -Z_{\mathrm{dH}}\left[1-\frac{Z_{\mathrm{dH}}}{10}\right]\left[\frac{12}{n}\right]^{1/2}\frac{28.1}{\pi}\frac{\bar{h}^2 r^3_{\mathrm{dH}}}{mr^5}. \tag{35}$$

Here $\phi^{\mathrm{FE}}_{\mathrm{HH}}(r)$ is the free electron contribution, $\phi^{c}_{\mathrm{HH}}(r)$ arises from the shift in the d band center due to s–d hybridization and ϕ^{b}_{HH} arises from the finite d-bandwidth. Z_{sH} and Z_{dH} are the number of s and d conduction electrons per host atom, κ is the Thomas Fermi screening constants, r_{cH} is the Ashcroft model-potential core radius and r_{dH} are the d state radii. n is the number of 1NNs of the host lattice and m is the mass of the electron.

Equations (32)–(35) are generalized to write the interatomic potential for the impurity–host interaction in the dilute alloys, which is given as [3]

$$\phi_{\mathrm{IH}}(r) = \phi^{FE}_{\mathrm{IH}}(r) + \phi^{c}_{\mathrm{IH}}(r) + \phi^{b}_{\mathrm{IH}}(r) \tag{36}$$

where

$$\phi^{FE}_{\mathrm{IH}}(r) = Z_{\mathrm{sH}}Z_{\mathrm{sI}}e^2\cosh(\kappa' r_{\mathrm{cH}})\cosh(\kappa' r_{\mathrm{cI}})\frac{\exp(-\kappa' r)}{r} \tag{37}$$

$$\phi^{c}_{\mathrm{IH}}(r) = Z^{\mathrm{eff}}_{\mathrm{d}}\frac{225}{\pi^2}\frac{\bar{h}^2 r^3_{\mathrm{dH}} r^3_{\mathrm{dI}}}{mr^8} \tag{38}$$

and

$$\phi^{b}_{\mathrm{IH}}(r) = -Z^{\mathrm{eff}}_{\mathrm{d}}\left[1-\frac{Z^{\mathrm{eff}}_{\mathrm{d}}}{10}\right]\left[\frac{12}{n}\right]^{1/2}\frac{28.1}{\pi}\frac{\bar{h}^2 r^{3/2}_{\mathrm{dH}} r^{3/2}_{\mathrm{dI}}}{mr^5}. \tag{39}$$

Here Z_{sI} and $Z^{\mathrm{eff}}_{\mathrm{d}}$ are the number of s conduction electrons and effective quasilocalized d-electron per impurity atom. r_{dI} is the d-state radius, r_{cI} is the Ashcroft model-potential core radius for the impurity and κ' is the Thomas Fermi screening length for host–impurity interaction. It is difficult to know the variation of the number of d electrons in the d-band by the introduction of an impurity. Therefore, we take the effective number of d electrons, $Z^{\mathrm{eff}}_{\mathrm{d}}$, in an alloy as the weighted average of the number of d electrons in the host and impurity atoms, i.e.,

$$Z^{\mathrm{eff}}_{\mathrm{d}} = C_{\mathrm{H}}Z_{\mathrm{dH}} + C_{\mathrm{I}}Z_{\mathrm{dI}} \tag{40}$$

where Z_{dI} is the number of quasilocalized d electrons per impurity atom and C_{H} and C_{I} are the concentrations of host and impurity atoms respectively.

In the alloying process, there may be further transfer of electrons to or from the s and d bands, as a result of which the conduction electron charge would redistribute around the impurity to screen or unscreen it. However, we assume that these charge transfers are small and we write the excess interatomic potential due to impurity as

$$\Delta\phi(r) = \Delta\phi^{\mathrm{FE}}(r) + \Delta\phi^{c}(r) + \Delta\phi^{b}(r) \tag{41}$$

where

$$\Delta\phi^{\mathrm{FE}}(r) = \frac{Z_{\mathrm{sH}}e^2}{r}\left[Z_{\mathrm{sI}}\cosh(\kappa' r_{\mathrm{cH}})\cosh(\kappa' r_{\mathrm{cI}})\exp(-\kappa' r) - Z_{\mathrm{sH}}\cosh^2(\kappa r_{\mathrm{cH}})\exp(-\kappa r)\right], \tag{42}$$

$$\Delta\phi^{c}(r) = \left[Z_{\mathrm{d}}^{\mathrm{eff}} r_{\mathrm{dI}}^3 - Z_{\mathrm{dH}} r_{\mathrm{dH}}^3\right]\frac{225}{\pi^2}\frac{\hbar^2 r_{\mathrm{dH}}^3}{m r^8}, \tag{43}$$

and

$$\Delta\phi^{b} r = \left[-Z_{\mathrm{d}}^{\mathrm{eff}}\left(1 - \frac{Z_{\mathrm{d}}^{\mathrm{eff}}}{10}\right) r_{\mathrm{dI}}^{3/2} + Z_{\mathrm{dH}}\left(1 - \frac{Z_{\mathrm{dH}}}{10}\right) r_{\mathrm{dH}}^{3/2}\right]\left[\frac{12}{n}\right]^{1/2}\frac{28.1}{\pi}\frac{\hbar^2 r_{\mathrm{dH}}^{3/2}}{m r^5}. \tag{44}$$

In eqs (41) to (44), $\Delta\phi^{\mathrm{FE}}(r)$, $\Delta\phi^{c}(r)$ and $\Delta\phi^{b}(r)$ are impurity induced changes in the potential due to free electron, s–d hybridization and d-bandwidth contributions respectively.

3. Calculations and results

The above formalism is used to calculate the atomic displacements in Ni and Pd dilute alloys due to 3d (Fe, Co, Ni and Cu), 4d (Nb, Mo and Pd) and 5d (W, Pt and Au) transition metal impurities. The physical parameters and a few calculated results are given in tables 1 and 2. The host potential $\phi_{\mathrm{HH}}(r)$ along with its constituents, for Ni and Pd metals are shown in figures 2 and 3 respectively. $\phi^{\mathrm{FE}}(r)$ and $\phi^{c}(r)$ are repulsive and $\phi^{b}(r)$ is attractive. The minima of $\Phi_{\mathrm{HH}}(r)$ for Ni and Pd metals are nearly at $r = 6.2$ a.u. which is more than the 1NN distance of 4.7 a.u. in Ni and 5.2 a.u. in Pd.

The change in potential $\Delta\phi(r)$ due to impurities in Ni and Pd metals are shown in figures 4 and 5 respectively. Here $\Delta\phi(r)$ depends upon impurity induced s–d hybridization and shift in the d band center which depends on the difference between Ashcroft core radius and d-state radius of the impurity and the host. In the dilute alloys of Ni, $\Delta\phi(r)$ for 3d impurities is smaller by an order of magnitude than those for 4d and 5d impurities as it is shown in the inset. $\Delta\phi(r)$ is repulsive at small distances and become attractive at large distances except for Cu impurity where it has just opposite character. However, in the dilute alloys of Pd, $\Delta\phi(r)$ is attractive at small distances and repulsive at large distances for all the 3d impurities, while for 4d impurities Nb and Mo, its behavior is the same as for

Table 1. The physical parameters (in a.u.) of Ni and Pd metals.

Host	a	Ω_0	Z	A_1 (10^{-3})	B_1 (10^{-3})
Ni	6.65	90	10	13.939	−6.855
Pd	7.35	99.3	10	20.033	−7.814

a is the lattice parameter, Ω_0 is the atomic volume, Z is the number of s and d conduction electrons per atom and A_1, B_1 are force constants as defined in eq. (15).

Table 2. Some calculated values of Ni and Pd metals.

			Ni			Pd		
Imp.	r_c (a.u.)	r_d (a.u.)	F_I (10^{-3})	F_{II} (10^{-3})	E_r $(-10^{-3}$ eV)	F_I (10^{-3})	F_{II} (10^{-3})	E_r $(-10^{-3}$ eV)
Fe	1.34	1.51	0.619	0.131	0.124	−4.892	0.261	0.601
Co	1.55	1.70	1.089	0.059	0.441	−3.064	0.275	1.252
Ni	1.00	1.34				−4.892	0.261	3.176
Cu	0.87	1.27	−1.407	−0.028	0.779	−6.083	0.268	4.896
Nb	1.91	2.42	−6.125	−0.109	14.199	11.763	0.648	18.285
Mo	1.79	2.27	−0.461	0.441	0.659	11.386	0.486	17.112
Pd	0.98	1.77	2.064	−0.365	2.521			
Pt	0.62	1.97	2.064	−0.668	7.838	−10.128	2.268	14.380
Au	0.76	1.91	1.573	−0.518	6.482	3.101	0.035	1.268

r_c and r_d are the Ashcroft core radius and d state radius respectively, F_I and F_{II} (in a.u.) are impurity-induced forces evaluated at 1NN's and 2NN's in the second approximation and E_r is the relaxation energy.

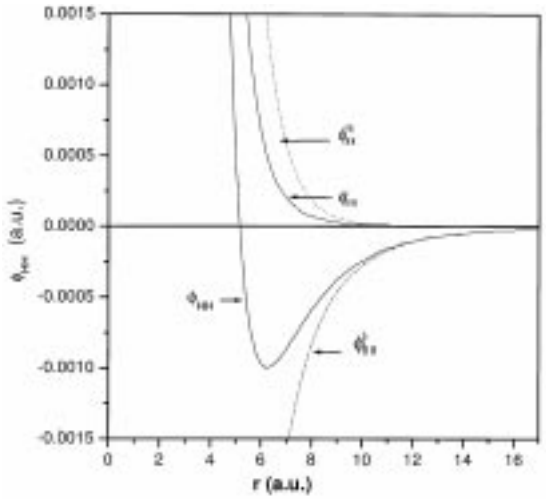

Figure 2. Interatomic potential $\phi_{HH}(r)$ for Ni metal. The description of ϕ^{FE}_{HH}, ϕ^{c}_{HH} and ϕ^{b}_{HH} is the same as given in the text.

Ni alloys. $\Delta\phi(r)$ for PdPt is similar to that of NiPt and behavior of PdAu is the same as that for NiAu alloy. It is to be noticed that the magnitude of $\Delta\phi(r)$ for PdAu is larger by two orders of magnitude than other alloys as shown in the inset.

The calculated $\Delta\phi(r)$ is used in eq. (31) to calculate F_I and F_{II} at the 1NN and 2NN of impurity in the second approximation. These values of F_I and F_{II} which are sensitive to the slope of $\Delta\phi(r)$ are given in table 2. In the Ni host, the forces are repulsive at 1NN's and attractive at 2NN's for Pd, Pt and Au impurities and for Mo impurity the forces are attractive for 1NN's and repulsive at 2NN's. For Cu and Nb impurities in Ni, the forces are attractive at the 1NN's and 2NN's while forces are repulsive for Fe and Co impurities

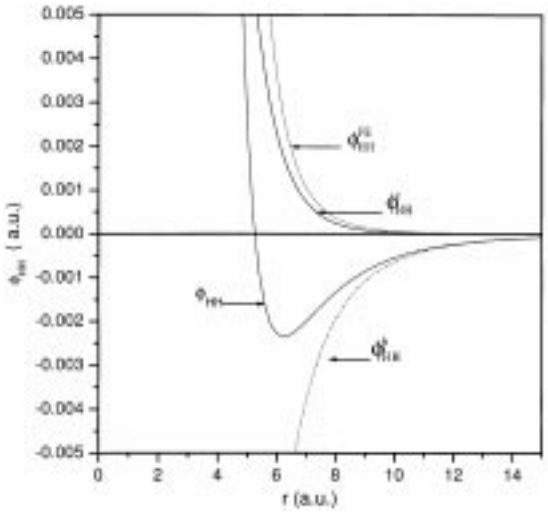

Figure 3. Interatomic potential $\phi_{\mathrm{HH}}(r)$ for Pd metal. The description of $\phi^{\mathrm{FE}}_{\mathrm{HH}}$, ϕ^{c}_{HH} and ϕ^{b}_{HH} is the same as given in figure 2.

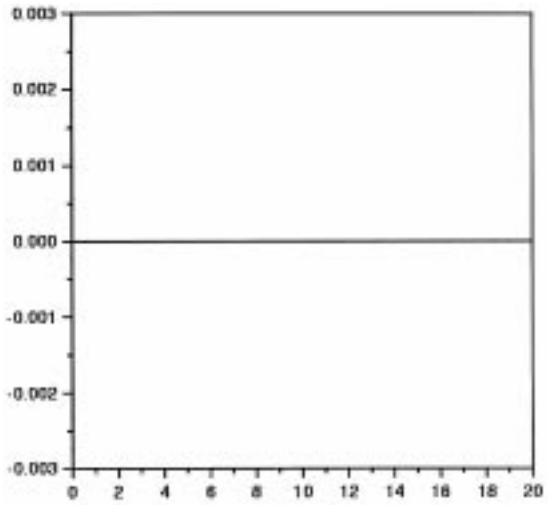

Figure 4.

at both the 1NN's and 2NN's. The forces are attractive at the first NN's and repulsive at the second NN's of impurity for Fe, Co, Ni, Cu, and Pt impurities in the Pd metal, whereas the forces are repulsive at 1NN's and 2NN's for Mo, Nb and Au impurities.

These values of F_{I} and F_{II}, and the calculated values of force constants A_1 and B_1, are used to calculate $\phi_{\alpha\alpha}(\vec{q})$ and hence $\vec{Q}(\vec{q})$ with the help of eqs (20)–(27). The inverse Fourier

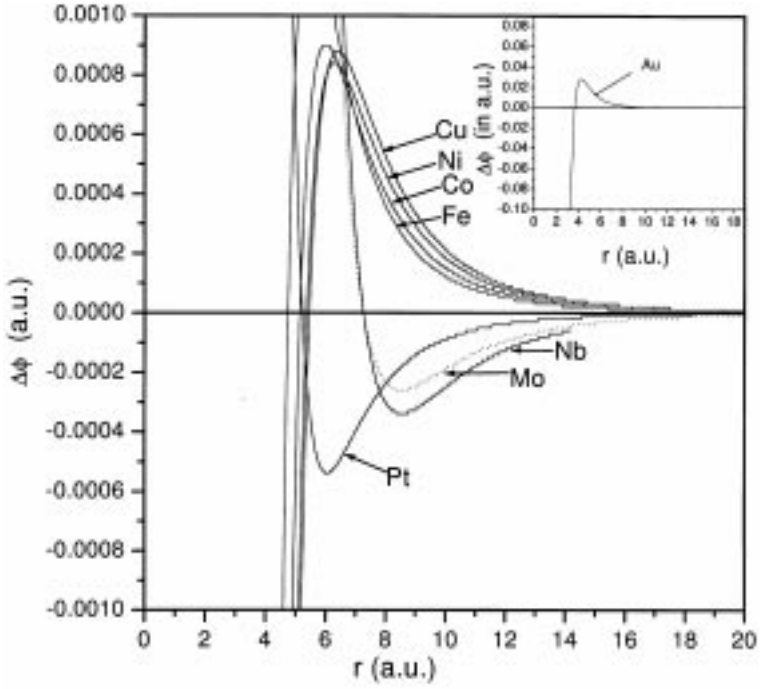

Figure 5. $\Delta\phi(r)$ vs. r for Fe, Co, Ni, Cu, Nb, Mo, Pt and Au impurities in Pd.

transform of $\vec{Q}(\vec{q})$, as given in eq. (5) gives $\vec{u}(\vec{R}_n^0)$. The numerical calculations are simplified by replacing the sum over $\vec{q}$ by the integration over the cube of edge $4\pi/a$ which inscribes the first Brillouin zone and using the fact that

$$\int_{\mathrm{BZ}} F(q)\,\mathrm{d}q = \frac{1}{2}\int_{\mathrm{cube}} F(q)\mathrm{d}q \tag{45}$$

for the fcc structure. The integration is carried out by Gaussian quadrature method. The calculated values of atomic displacements are tabulated in tables 3 to 6 for Ni(Fe, Co, Cu, Nb, Mo, Pd, Au and Pt) dilute alloys and tables 7 to 10 for Pd(Fe, Co, Cu, Ni, Mo, Nb, Au and Pt) dilute alloys respectively. These displacements are oscillatory in nature and are significant even up to 25 nearest neighbors of impurity which are tabulated here. The displacements are calculated up to five decimal places but due to space economy, the numbers are tabulated up to second decimal places. Interested readers may have the detailed data from the author.

In the NiFe dilute alloy the 1NN's displace away from the impurity, the 2NN's displace towards impurity atom, and third and fourth NN's displace away from the impurity , which are followed by oscillatory nature of displacements. The maximum $|u(r)|$ due to Fe is found at 1NN's site. The (310), (321) and (411) NN's show that the anisotropic displacements and atomic displacements due to Co impurity are the same as for Fe impurity except that $|u(r)|$ is maximum at the 2NN's site. For Fe and Co impurities the displacements of NN's which move away from the impurity are larger than those which move towards the

impurity and therefore the lattice expands. The displacements due to Cu, Nb and Mo impurities are isotropic as well as anisotropic. The $|u(r)|$ is maximum at 2NN's. The 1NN's displace towards the impurity atom, 2NN's displace away from the impurity atom, third and fourth NN's show contraction towards impurity and further displacements are oscillatory in nature and decreasing in magnitude. The $|u(r)|$ towards the impurity atom are larger than away from the impurity. Therefore the lattice shows contraction. The 1NN's of Pd, Pt and Au impurities are displaced away from the impurity, 2NN's show contraction and third and fourth NN's are displaced away from the impurity atom. The displacements are maximum at the 2NN's.

The magnitude of atomic displacements for Ni alloys up to 5NN's are shown in figure 6. The strain field increases with the increase in d electrons for 3d impurities. For 4d impurities the strain is maximum for Nb impurity and decreases for Mo impurity and again increases for Pd impurity. The strain field for 5d impurity Pt and Au is nearly the same. The maximum displacement of 4.6% of R_1^0 is found for NiNb alloy while minimum displacement of 0.63% of R_1^0 is for NiFe alloy.

The calculated atomic displacement of the 1NN's for Fe, Pd, Pt and Au impurities in Ni show lattice expansion of 0.0298 a.u., 0.87 a.u., 0.84 a.u and 0.86 a.u. at 1NN's, whereas

Table 3. Atomic displacements (in 10^{-2} a.u.) of the NN's of Fe and Co impurities in Ni.

NN's	Fe			Co		
(n_1, n_2, n_3)	u_x	u_y	u_z	u_x	u_y	u_z
110	1.40	1.40	0.00	2.67	2.67	0.00
200	−1.27	0.00	0.00	−3.32	0.00	0.00
211	0.18	0.18	0.18	0.25	0.27	0.27
220	0.81	0.81	0.00	1.72	1.72	0.00
310	0.02	−0.26	0.00	−0.19	−0.58	0.00
222	−0.41	−0.41	−0.41	−1.04	−1.04	−1.04
321	0.41	−0.27	0.25	0.82	−0.63	0.68
400	0.50	0.00	0.00	0.63	0.00	0.00
411	1.14	−0.45	−0.45	2.34	−1.15	−1.15
330	−0.28	−0.28	0.00	−0.71	−0.71	0.00
420	0.39	1.08	0.00	0.60	2.42	0.00
332	−0.27	−0.27	0.01	−0.59	−0.59	0.11
422	0.73	−0.40	−0.40	1.73	−1.08	−1.08
431	−0.23	0.11	0.70	−0.62	0.20	1.67
510	0.16	0.02	0.00	0.26	−0.17	0.00
521	0.35	0.96	−0.16	0.70	2.01	−0.64
440	−1.07	−1.07	0.00	−2.51	−2.51	0.00
433	−0.17	−0.01	−0.01	−0.33	−0.02	−0.02
530	0.49	1.25	0.00	0.87	2.86	0.00
442	0.33	0.33	−0.56	0.84	0.84	−1.42
600	0.55	0.00	0.00	1.41	0.00	0.00
611	−0.91	−0.46	−0.46	−2.06	−1.20	−1.20
532	−0.30	0.25	0.46	−0.80	0.40	0.85
620	−0.53	1.07	0.00	−1.20	2.54	0.00
541	0.48	−0.41	0.29	1.16	−0.99	0.57

The coordinates (n_1, n_2, n_3) of the NN's are in units of $(a/2)$ and (u_x, u_y, u_z) are Cartesian components of atomic displacements here and in the subsequent tables.

Table 4. Atomic displacements (in 10^{-2} a.u.) of the NN's of Cu and Nb impurities in Ni.

NN's	Cu			Nb		
(n_1, n_2, n_3)	u_x	u_y	u_z	u_x	u_y	u_z
110	−3.51	−3.51	0.00	−15.29	−15.29	0.00
200	4.59	0.00	0.00	20.10	0.00	0.00
211	−0.31	−0.34	−0.34	−1.34	−1.48	−1.48
220	−2.30	−2.30	0.00	−10.05	−10.05	0.00
310	0.30	0.78	0.00	1.34	3.40	0.00
222	1.44	1.44	1.44	6.29	6.29	6.29
321	−1.09	0.85	−0.94	−4.77	3.72	−4.12
400	−0.75	0.00	0.00	−3.24	0.00	0.00
411	−3.11	1.59	1.59	−13.58	6.97	6.97
330	0.98	0.98	0.00	4.30	4.30	0.00
420	−0.76	−3.28	0.00	−3.29	−14.35	0.00
332	0.80	0.80	−0.17	3.51	3.51	−0.74
422	−2.36	1.50	1.50	−10.31	6.59	6.59
431	0.87	−0.27	−2.28	3.81	−1.17	−9.95
510	−0.32	0.28	0.00	−1.40	1.22	0.00
521	−0.93	−2.69	0.93	−4.06	−11.76	4.07
440	3.43	3.43	0.00	14.99	14.99	0.00
433	0.43	0.03	0.03	1.89	0.14	0.14
530	−1.13	−3.89	0.00	−4.90	−17.00	0.00
442	−1.15	−1.15	1.96	−5.04	−5.04	8.59
600	−1.94	0.00	0.00	−8.51	0.00	0.00
611	2.79	1.66	1.66	12.21	7.28	7.28
532	1.11	−0.50	−1.10	4.86	−2.19	−4.81
620	1.63	−3.47	0.00	7.13	−15.16	0.00
541	−1.59	1.35	−0.75	−6.96	5.91	−3.26

Table 5. Atomic displacements (in 10^{-2} a.u.) of the NN's of Mo and Pd impurities in Ni.

NN's	Mo			Pd		
(n_1, n_2, n_3)	u_x	u_y	u_z	u_x	u_y	u_z
110	−1.70	−1.70	0.00	6.20	6.20	0.00
200	4.39	0.00	0.00	−10.09	0.00	0.00
211	0.05	0.01	0.01	0.37	0.44	0.44
220	−1.52	−1.52	0.00	4.44	4.44	0.00
310	0.67	0.58	0.00	−1.01	−1.56	0.00
222	1.33	1.33	1.33	−3.12	−3.12	−3.12
321	−0.61	0.67	−0.92	2.01	−1.74	2.08
400	0.39	0.00	0.00	0.64	0.00	0.00
411	−1.91	1.49	1.49	5.86	−3.47	−3.47
330	0.92	0.92	0.00	−2.14	−2.14	0.00
420	−0.04	−2.49	0.00	1.04	6.62	0.00
332	0.59	0.59	−0.31	−1.60	−1.60	0.50
422	−1.94	1.50	1.50	4.89	−3.36	−3.36
431	0.87	−0.14	−1.89	−1.95	0.48	4.74
510	−0.04	0.63	0.00	0.46	−0.94	0.00
521	−0.54	−1.75	1.25	1.73	5.16	−2.36
440	2.82	2.82	0.00	−7.12	−7.12	0.00
433	0.22	0.03	0.03	−0.77	−0.07	−0.07
530	−0.41	−3.06	0.00	1.86	7.94	0.00
442	−1.04	−1.04	1.82	2.47	2.47	−4.26
600	−1.82	0.00	0.00	4.23	0.00	0.00
611	2.14	1.60	1.60	−5.65	−3.66	−3.66
532	1.08	−0.07	−0.47	−2.46	0.73	1.89
620	1.26	−2.89	0.00	−3.31	7.23	0.00
541	−1.35	1.15	−0.38	3.34	−2.84	1.34

Table 6. Atomic displacements (in 10^{-2} a.u.) of the NN's of Pt and Au impurities in Ni.

NN's	Pt			Au		
(n_1, n_2, n_3)	u_x	u_y	u_z	u_x	u_y	u_z
110	5.99	5.99	0.00	6.09	6.09	0.00
200	−11.24	0.00	0.00	−10.96	0.00	0.00
211	0.22	0.30	0.30	0.26	0.35	0.35
220	4.57	4.57	0.00	4.56	4.56	0.00
310	−1.34	−1.65	0.00	−1.25	−1.63	0.00
222	−3.46	−3.46	−3.46	−3.38	−3.38	−3.38
321	2.00	−1.86	2.34	2.02	−1.84	2.27
400	0.10	0.00	0.00	0.26	0.00	0.00
411	5.94	−3.86	−3.86	5.95	−3.76	−3.76
330	−2.38	−2.38	0.00	−2.32	−2.32	0.00
420	0.77	7.02	0.00	0.86	6.95	0.00
332	−1.68	−1.68	0.64	−1.67	−1.67	0.61
422	5.28	−3.79	−3.79	5.20	−3.68	−3.68
431	−2.19	0.47	5.13	−2.13	0.48	5.05
510	0.37	−1.25	0.00	0.40	−1.16	0.00
521	1.73	5.29	−2.84	1.74	5.29	−2.71
440	−7.68	−7.68	0.00	−7.56	−7.56	0.00
433	−0.76	−0.08	−0.08	−0.77	−0.08	−0.08
530	1.70	8.49	0.00	1.76	8.37	0.00
442	2.72	2.72	−4.72	2.66	2.66	−4.61
600	4.70	0.00	0.00	4.59	0.00	0.00
611	−6.01	−4.09	−4.09	−5.94	−3.98	−3.98
532	−2.75	0.58	1.78	−2.68	0.63	1.83
620	−3.53	7.83	0.00	−3.48	7.70	0.00
541	3.63	−3.09	1.31	3.57	−3.04	1.33

corresponding experimental observations show lattice expansion of 0.0038±0.0056 a.u., 0.98±0.006 a.u., 0.12±0.006 a.u. and 0.15±0.019 a.u. respectively [12]. The calculated $u(r)$ at 1NN due to Nb and Mo impurities show contraction and expansion at the 2NN's while the experimental results show the expansion at 2NN's. For Co impurity the calculated $u(r)$ gives expansion at the 1NN and contraction at the 2NN's while experimental results show contraction at the 1NN's. Due to large error bars in the experimental values, the comparison is inconclusive. However, the calculated and experimental results show that there is lattice expansion due to these impurities.

The 1NN's for Fe, Co, Ni and Cu impurities in Pd show contraction towards the impurity atom, 2NN's displace away from the impurity, and 3NN's displace towards impurity followed by oscillatory nature of displacements. The displacements are maximum at the 1NN's of all impurities. The first and second NN's of Nb and Mo impurities, displace away from the impurity and 3NN's show anisotropic displacements followed by an oscillatory nature of atomic displacements. The nature of $\vec{u}(\vec{r})$ for Pt impurity is the same as that for Ni impurity. However, for Au impurity, 1NN's move away from the impurity, 2NN's towards the impurity and 3NN's show anisotropic displacements.

The magnitude of atomic displacements for Pd alloys are shown in figure 7. The displacements due to 3d impurities increase with the increase in d electrons. For 4d impurities Nb and Mo, the strain is nearly the same while for 5d impurities strain decreases from Pt to Au. The maximum displacement of 3.8% of R_1^0 is found for PdNb alloy while the

Table 7. Atomic displacements (in 10^{-2} a.u.) of the NN's of Fe and Co impurities in Pd.

NN's	Fe			Co		
(n_1, n_2, n_3)	u_x	u_y	u_z	u_x	u_y	u_z
110	−0.85	−0.85	0.00	−2.58	−2.58	0.00
200	0.64	0.00	0.00	0.60	0.00	0.00
211	−0.13	0.44	0.44	−0.41	1.11	1.11
220	0.01	0.01	0.00	−0.12	−0.12	0.00
310	−1.26	0.06	0.00	−3.35	0.06	0.00
222	1.03	1.03	1.03	2.71	2.71	2.71
321	0.02	0.37	0.17	−0.01	0.99	0.47
400	−0.18	0.00	0.00	−0.86	0.00	0.00
411	−0.86	−1.05	−1.05	−2.44	−2.52	−2.52
330	0.50	0.50	0.00	1.22	1.22	0.00
420	−1.02	−0.30	0.00	−2.65	−0.80	0.00
332	0.88	0.88	0.47	2.38	2.38	1.36
422	−0.25	−0.57	−0.57	−0.61	−1.26	−1.26
431	0.14	0.50	0.31	0.36	1.26	0.73
510	0.82	0.09	0.00	1.70	0.03	0.00
521	−0.85	−0.59	−0.36	−2.20	−1.58	−0.97
440	0.21	0.21	0.00	0.56	0.56	0.00
433	0.48	−0.02	−0.02	1.44	0.24	0.24
530	−0.54	−1.04	0.00	−1.41	−2.51	0.00
442	1.09	1.09	0.43	2.78	2.78	1.09
600	−0.36	0.00	0.00	−0.61	0.00	0.00
611	0.40	0.79	0.79	0.96	1.71	1.71
532	−0.29	0.03	−0.19	−0.69	0.10	−0.46
620	0.85	−0.38	0.00	1.89	−1.04	0.00
541	0.21	0.13	−0.94	0.50	0.38	−2.22

Table 8. Atomic displacements (in 10^{-2} a.u.) of the NN's of Ni and Cu impurities in Pd.

NN's	Ni			Cu		
(n_1, n_2, n_3)	u_x	u_y	u_z	u_x	u_y	u_z
110	−4.11	−4.11	0.00	−5.11	−5.11	0.00
200	0.62	0.00	0.00	0.66	0.00	0.00
211	−0.66	1.71	1.71	−0.82	2.10	2.10
220	−0.23	−0.23	0.00	−0.30	−0.30	0.00
310	−5.23	0.07	0.00	−6.47	0.08	0.00
222	4.23	4.23	4.23	5.22	5.22	5.22
321	−0.03	1.56	0.73	−0.04	1.93	0.91
400	−1.46	0.00	0.00	−1.85	0.00	0.00
411	−3.84	−3.86	−3.86	−4.76	−4.74	−4.74
330	1.86	1.86	0.00	2.29	2.29	0.00
420	−4.12	−1.25	0.00	−5.09	−1.55	0.00
332	3.72	3.72	2.15	4.61	4.61	2.67
422	−0.94	−1.89	−1.89	−1.16	−2.31	−2.31
431	0.55	1.93	1.10	0.68	2.38	1.36
510	2.50	−0.02	0.00	3.05	−0.04	0.00
521	−3.42	−2.48	−1.52	−4.22	−3.06	−1.88
440	0.87	0.87	0.00	1.08	1.08	0.00
433	2.29	0.45	0.45	2.84	0.58	0.58
530	−2.19	−3.84	0.00	−2.71	−4.72	0.00
442	4.29	4.29	1.69	5.29	5.29	2.08
600	−0.86	0.00	0.00	−1.03	0.00	0.00
611	1.47	2.56	2.56	1.80	3.12	3.12
532	−1.05	0.16	−0.70	−1.30	0.20	−0.86
620	2.85	−1.62	0.00	3.48	−2.01	0.00
541	0.77	0.61	−3.38	0.94	0.76	−4.15

Table 9. Atomic displacements (in 10^{-2} a.u.) of the NN's of Nb and Mo impurities in Pd.

NN's	Nb			Mo		
(n_1, n_2, n_3)	u_x	u_y	u_z	u_x	u_y	u_z
110	9.87	9.87	0.00	9.56	9.56	0.00
200	0.94	0.00	0.00	0.64	0.00	0.00
211	1.61	−3.66	−3.66	1.56	−3.59	−3.59
220	0.83	0.83	0.00	0.77	0.77	0.00
310	11.75	0.05	0.00	11.46	0.02	0.00
222	−9.42	−9.42	−9.42	−9.20	−9.20	−9.20
321	0.21	−3.53	−1.68	0.19	−3.44	−1.64
400	4.12	0.00	0.00	3.92	0.00	0.00
411	8.91	8.05	8.05	8.66	7.92	7.92
330	−3.90	−3.90	0.00	−3.83	−3.83	0.00
420	9.13	2.82	0.00	8.92	2.75	0.00
332	−8.40	−8.40	−5.04	−8.19	−8.19	−4.89
422	2.02	3.71	3.71	1.98	3.68	3.68
431	−1.21	−4.15	−2.27	−1.18	−4.07	−2.24
510	−4.55	0.51	0.00	−4.57	0.44	0.00
521	7.52	5.57	3.43	7.35	5.43	3.34
440	−1.97	−1.97	0.00	−1.92	−1.92	0.00
433	−5.44	−1.62	−1.62	−5.27	−1.50	−1.50
530	4.87	8.04	0.00	4.76	7.91	0.00
442	−9.33	−9.33	−3.68	−9.14	−9.14	−3.61
600	1.22	0.00	0.00	1.27	0.00	0.00
611	−3.04	−4.90	−4.90	−3.00	−4.88	−4.88
532	2.20	−0.41	1.49	2.16	−0.40	1.47
620	−5.59	3.69	0.00	−5.55	3.60	0.00
541	−1.62	−1.46	6.96	−1.59	−1.41	6.87

Table 10. Atomic displacements (in 10^{-2} a.u.) of the NN's of Pt and Au impurities in Pd.

NN's	Pt			Au		
(n_1, n_2, n_3)	u_x	u_y	u_z	u_x	u_y	u_z
110	−8.53	−8.53	0.00	2.60	2.60	0.00
200	4.57	0.00	0.00	−0.01	0.00	0.00
211	−1.32	4.13	4.13	0.42	−1.01	−1.01
220	−0.12	−0.12	0.00	0.19	0.19	0.00
310	−11.98	0.42	0.00	3.19	−0.01	0.00
222	9.77	9.77	9.77	−2.56	−2.56	−2.56
321	0.11	3.51	1.62	0.04	−0.95	−0.45
400	−2.22	0.00	0.00	1.02	0.00	0.00
411	−8.39	−9.65	−9.65	2.38	2.25	2.25
330	4.63	4.63	0.00	−1.09	−1.09	0.00
420	−9.60	−2.85	0.00	2.49	0.76	0.00
332	8.46	8.46	4.64	−2.27	−2.27	−1.34
422	−2.30	−5.05	−5.05	0.56	1.07	1.07
431	1.30	4.69	2.82	−0.33	−1.15	−0.64
510	7.17	0.58	0.00	−1.36	0.08	0.00
521	−8.01	−5.65	−3.44	2.06	1.51	0.93
440	1.97	1.97	0.00	−0.53	−0.53	0.00
433	4.81	0.21	0.21	−1.44	−0.37	−0.37
530	−5.09	−9.55	0.00	1.33	2.25	0.00
442	10.23	10.23	4.00	−2.56	−2.56	−1.01
600	−2.94	0.00	0.00	0.41	0.00	0.00
611	3.69	6.98	6.98	−0.85	−1.42	−1.42
532	−2.65	0.28	−1.71	0.62	−0.11	0.41
620	7.59	−3.65	0.00	−1.61	1.00	0.00
541	1.89	1.27	−8.57	−0.45	−0.39	1.96

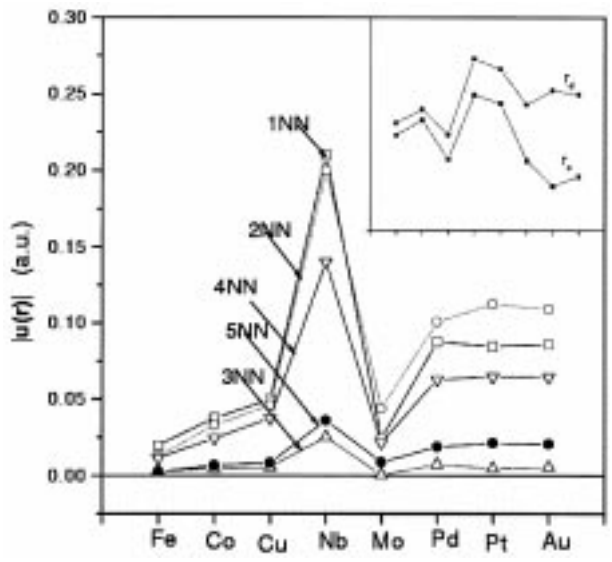

Figure 6. Magnitude of the displacements $|u(r)|$ as function of atomic number of the impurity in Ni metal. The inset figure shows Ashcroft core radii (r_c) and d core radius (r_d) of impurities in the same order mentioned in *x*-axis. The lines joining the points are for visual guidance.

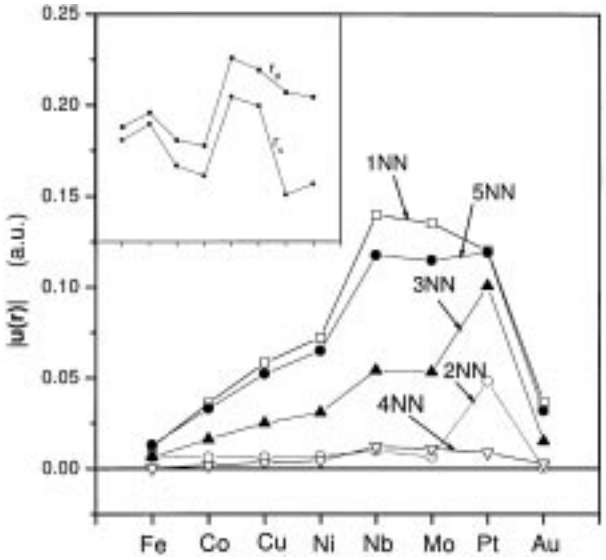

Figure 7. Magnitude of the displacements $|u(r)|$ as function of atomic number of the impurity in Pd metal. The inset figure shows Ashcroft core radii (r_c) and d core radius (r_d) of impurities in the same order mentioned in *x*-axis. The lines joining the points are for visual guidance.

minimum displacement of 0.23% of R_1^0 is for PdFe alloy. The calculated atomic displacements of Fe, Co, Ni, Cu and Pt show the lattice contraction of 0.0126 a.u., 0.036 a.u., 0.058 a.u., 0.072 a.u. and 0.12a.u. at the 1NN's respectively whereas the corresponding experimental observations show lattice contraction of 0.054±0.002 a.u., 0.073±0.013 a.u., 0.096±0.019 a.u., 0.115±0.008 a.u. and 0.021±0.019 a.u. respectively. The calculated lattice expansion for Au impurity in Pd is 0.036 a.u. whereas the experimental results [12] show the expansion of 0.017 a.u.±0.015 a.u. The calculated results for the first two NN's of Nb and Mo impurities show the expansion while the experimental results show the contraction with large error bars. Therefore, comparison remains inconclusive and further careful investigations are needed.

To find a general behavior of atomic displacement in Ni and Pd alloys, the Ashcroft and d core radii r_{cI} and r_{dI} are also plotted in figures 6 and 7 on arbitrary scale. We note that except for Cu, the variation of atomic displacements is the same as that of core radii. The calculated atomic displacements up to 2NN's are used to calculate the impurity induced relaxation energy E_{r} which is given as

$$E_{\mathrm{r}} = -\frac{1}{2}\sum_{n\alpha} F_{n\alpha} u_{n\alpha}. \tag{46}$$

Here $\vec{F}$ is isotropic and the values of F_{I} and F_{II} tabulated in table 2 are used in eq. (46). The result for E_{r} are also given in table 2. The relaxation energies are of the order of meV which have very small values and the accuracy of these values depends on the impurity induced forces and the atomic displacements. The input parameters are accurate within 1% and therefore the relaxation energy also have the same accuracy. The relaxation energies for Fe, Co, Cu, and Mo are smaller than other impurities. Therefore, these impurities may be easily dissolved in Ni. However, in the case of Pd the relaxation energies for Fe, Co and Au impurities are smaller than other impurities, and these may be easily be dissolved.

4. Discussion

We have used here Wills and Harrison model potential [3] for the host Ni and Pd metals and other transition metal impurities. The effect of partially localized d electrons is included through d bandwidth and s–d hybridization. The host potential $\phi_{\mathrm{HH}}(r)$ and change in potential due to impurity $\Delta\phi(r)$ are very small and smooth beyond 2NN distance. Therefore, the contribution to $\phi_{\alpha\beta}(q)$ and $F_\alpha(q)$ are expected to be small beyond 2NN's. In the present calculations, it is assumed that the impurity is screened by Fermi–Thomas screening and therefore Fridel oscillations are absent. In the numerical calculations the cubic symmetry of the lattice is retained although the exact anisotropy of the Brillouin zone is not accounted for. This may not introduce serious error considering other simplifications in the calculations. The calculated values of the atomic displacements in Ni and Pd alloys agree qualitatively with the observed experimental data. The calculated values of atomic displacements in Ni and Pd dilute alloys are found to be proportional to s and d core radii of impurities. The tabulated values of displacements may be quite useful to investigate heat of solution, electric field gradients, asymmetry parameter, wipe out number, Knight shift and other properties of the defect lattice where impurity induced displaced positions of the host atoms in dilute alloys of Pd and Ni are needed. This will help in basic understanding

of the alloy formation. Further, this study will explain the strength at high temperature, high stiffness, low coefficient of thermal expansion and chemical compatibility in a variety of environments.

Acknowledgement

The financial support from University Grant Commission (UGC), New Delhi is gratefully acknowledged.

References

[1] J Singh, P Singh, S K Rattan and S Prakash, *Phys. Rev.* **B49**, 932 (1994)
[2] Hitesh Sharma and S Prakash, *Can. J. Phys.* (2002) (accepted)
[3] J M Wills and W A Harrison, *Phys. Rev.* **B28**, 4363 (1983)
[4] P Singh, S Prakash and J Singh, *Phys. Rev.* **B49**, 12259 (1994)
[5] A Gordon and S Dorfman, *Phys. Rev.* **B51**, 930 (1995)
[6] D Fucks and S Dorfman, *Phys. Rev.* **B55**, 3461 (1997)
[7] P Singh and S Prakash, *Phys. Rev.* **B59**, 14226 (1999)
[8] W Hanke, *Phys. Rev.* **B8**, 4585, 4591 (1973)
[9] J Singh, N Singh and S Prakash, *Phys. Rev.* **B12**, 3159 (1975); **12**, 3166 (1975); **18**, 2954 (1978)
[10] J Singh and S Prakash, *Nuovo Cimento* **37**, 131 (1977)
[11] Kanzaki, *J. Phys. Chem. Solids* **2**, 24 (1957)
[12] U Scheuer and B Lengeler, *Phys. Rev.* **B44**, 9883 (1991)